



## Theoretical design of highly luminescent europium (III) complexes: A factorial study

José Diogo L. Dutra, Iara F. Gimenez, Nivan B. da Costa Junior, Ricardo O. Freire\*

Departamento de Química, UFS, 49100-000 São Cristóvão, SE, Brazil

### ARTICLE INFO

#### Article history:

Received 9 June 2010

Received in revised form 30 October 2010

Accepted 16 November 2010

Available online 23 November 2010

#### Keywords:

Design  
Sparkle/AM1  
Europium  
Luminescence

### ABSTRACT

In this work, the design of europium (III) complexes exhibiting high quantum yield was accomplished by a systematic study using factorial design and the Sparkle/AM1 model. Eight new complexes derived from the Eu(acac)<sub>3</sub>·o-phen complex (acac = acetylacetonate acid and o-phen = 1,10-phenanthroline) were generated through a 2<sup>3</sup> full factorial design. The ground state geometries of the eight new complexes were predicted using the Sparkle/AM1 model. The singlet and triplet excited levels were calculated using the INDO/S-CIS method, implemented in ZINDO program. Energy transfer rates and quantum yields for each one of the new complexes were calculated using the theoretical model based on the theory of the transitions 4f–4f (Spectrochim. Acta Part A, 1998, 54, 1593). The results strongly suggest that the europium complexes with β-diketone ligands might display a quantum yield increment when strongly electron acceptor groups are added to one of the β-diketone extremities and strongly electron donor groups are added to the opposite side. From the factorial design proposed in this work it was possible to project complexes with quantum yields up to 70%.

© 2010 Elsevier B.V. All rights reserved.

### 1. Introduction

The late 1990s witnessed an abrupt rise in the research on lanthanides owing to studies of lanthanide complexes as functional elements in the so-called light conversion molecular devices (LCMDs) [1]. Nowadays, lanthanide compounds find applications in many distinct devices such as chemical sensors, diagnostic systems, luminescent materials, and liquid crystals, to name a few [1–8]. The main advantages of luminescent lanthanides complexes with chelating ligands in comparison to traditional organic fluorophores are the long luminescence lifetimes in addition to narrow emission bands and low concentration quenching.

The development of complexes of lanthanide ions as efficient LCMDs has become an important theme in coordination chemistry, and in this context the theoretical strategy have proven to be successful in the design of efficient luminescent devices with lanthanide complexes [9,10]. From a theoretical point of view, previous works stated that the task of designing new efficient LCMDs can be accomplished by three steps: (1) optimization of the ground state geometry; (2) the calculation of the electronic excited states; and (3) the prediction of the emission quantum yield,  $q$  [11,12]. The last step is carried out by the calculation of the energy transfer rates

between the excited states of the lanthanide ion and the excited states of the ligands, followed by numerically solving a system of rate equations to give  $q$  [11].

The first step is very time-consuming compared to the two last ones but a careful geometry optimization is crucial for the quality of the prediction of spectroscopic properties. *Ab initio* and DFT calculations have been used by some research groups to predict the ground state geometries of lanthanide complexes [13–16]. In this context the use of the effective core potentials (ECP) [17,18] makes possible the calculation of the ground state geometry of the lanthanide complexes with high accuracy. However, application of this method to large systems is not convenient because a high computational time is required [19,20].

Semiempirical models, on the other hand, demand a lower computational effort and were found to provide an interesting alternative for the modeling of these compounds [21–24]. In particular, the semiempirical Sparkle/AM1 [25–31] and Sparkle/PM3 [32] models were developed for the calculation of the ground state geometries of the lanthanide complexes with great accuracy. Additionally the Sparkle/AM1 model is quite competitive with present day *ab initio*/ECP calculations, while being hundreds of times faster [25]. This feature can be very useful if one is interested in applying multivariate statistical techniques such as two-level factorial design [33,34], where several lanthanide complexes can be investigated.

In this work we applied the Sparkle/AM1 model to the design of novel Eu complexes with substituted β-diketone ligands,

\* Corresponding author. Departamento de Química, UFS, 49100-000 São Cristóvão, SE, Brazil. Tel.: +55 79 2105 6650; fax: +55 79 2105 6651.

E-mail address: [rfreire@ufs.br](mailto:rfreire@ufs.br) (R.O. Freire).

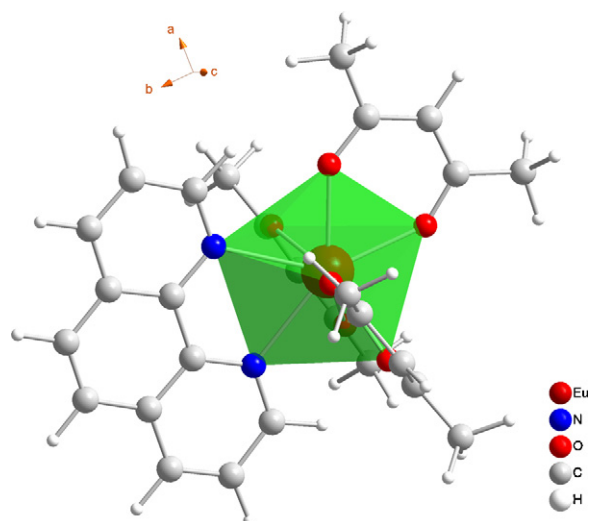


Fig. 1. Schematic three dimensional representation of the crystallographic structure of the tris(acetylacetonate)(1,10-phenanthroline)-europium(III) obtained from Cambridge Structural Database 2008 [37–39].

whose substitution followed a two-level factorial design. Among the reasons for the choice of  $\beta$ -diketonates are the applications of  $\beta$ -diketonate lanthanide complexes as emissive materials in OLEDs. These complexes are thermodynamically stable and highly soluble or volatile lanthanide complexes. Our major aim is to assist the development of a complex with optimized luminescent properties, avoiding a high number of practical experiments.

## 2. Computational procedure

Owing to potential applications in clinical analyses [35,36], a  $\beta$ -diketonate lanthanide complex (tris(acetylacetonate)(1,10-phenanthroline)-europium(III), Fig. 1 was chosen in this work as a substrate to systematic substitutions according to a  $2^3$  factorial planning. The initial structure was obtained from Cambridge Structural Database (CSD) [37–39]. The coordination polyhedron around the lanthanide ion in this complex is composed by six oxygen atoms from acetylacetonate ligands and two nitrogen atoms from 1,10-phenanthroline ligand.

Structure	R1	R2	R3
Comp01	NO <sub>2</sub>	H	CH <sub>3</sub>
Comp02	NH <sub>2</sub>	H	CH <sub>3</sub>
Comp03	NO <sub>2</sub>	CH <sub>3</sub> CH <sub>2</sub>	CH <sub>3</sub>
Comp04	NH <sub>2</sub>	CH <sub>3</sub> CH <sub>2</sub>	CH <sub>3</sub>
Comp05	NO <sub>2</sub>	H	CF <sub>3</sub>
Comp06	NH <sub>2</sub>	H	CF <sub>3</sub>
Comp07	NO <sub>2</sub>	CH <sub>3</sub> CH <sub>2</sub>	CF <sub>3</sub>
Comp08	NH <sub>2</sub>	CH <sub>3</sub> CH <sub>2</sub>	CF <sub>3</sub>

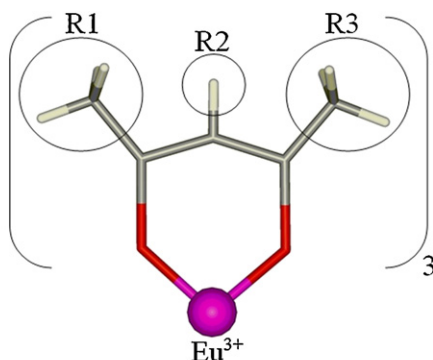


Fig. 2. Nomenclature used for the eight europium (III) complexes generated by the  $2^3$  factorial design and schematic representation of the precursor ligand present in the  $\text{Eu}^{3+}$  complexes investigated in this work.

The eight new structures resulting from  $2^3$  factorial planning were generated considering substitutions at R1, R2 and R3 positions of the acetylacetonate molecule, Fig. 2. The H atom at the R2 position was replaced by  $\text{CH}_3\text{CH}_2$  group in order to ensure a higher solubility in organic solvents. Donor and acceptor groups were chosen for substitution at the other positions in order to evaluate the effect of the chemical nature of the substituent on the energy transfer rate as well as on the quantum yield of lanthanide emission:  $\text{NO}_2$  (strong acceptor) and  $\text{NH}_2$  (strong donor) at R1 position and  $\text{CF}_3$  (strong acceptor) and  $\text{CH}_3$  (weak donor) at R3 position.

The resulting structures were subjected to calculation using the Sparkle model [25], implemented in the MOPAC2007 package [40]. The keywords used in the calculation reported in this work were: AM1; PRECISE; BFGS; GNORM=0.25; SCFCRT=1.D-10 (to increase the SCF convergence criterion) and XYZ (for Cartesian coordinates).

The ground state geometries predicted by Sparkle/AM1 model [25] were used as input in the calculation of the singlet and triplet excited states using configuration interaction single (CIS) based on the intermediate neglect of differential overlap/spectroscopic (INDO/S) technique [41,42] implemented in ZINDO program [43]. For the energy transfer rates between the ligands and the lanthanide ion and the emission quantum yield calculation we used the theoretical model based on the theory of the transitions  $4f-4f$  [11].

Some restrictions were taken into account in the calculation of the energy transfer rates and in the emission quantum yields. These restrictions were: (i) the oscillator strength of the transitions should be larger than 0.2; (ii) it was considered only the triplet state with the lowest energy, which is related to the singlet state chosen in item i; (iii) the singlet state must have energy below  $40,000.00\text{ cm}^{-1}$ ; and (iv) in the calculation of the energy transfer rate, the singlet (S) or triplet (T) states and the  $^5\text{D}_0$  or  $^5\text{D}_1$  levels should present an energy difference  $\Delta E = E(\text{S or T}) - E(^5\text{D}_j)$  below  $9000\text{ cm}^{-1}$ . These restrictions were based on experimental data (electronic spectra and energy transfer rate) taken from several lanthanide compounds found in the literature. The mechanism of energy transfer from the ligand triplet state to the  $^5\text{L}_6$  and  $^5\text{D}_1$  excited state of europium (III) ion adopted here can be observed in Fig. 3.

The Jablonski diagram presented in Fig. 3 shows the probable luminescence mechanism. The  $W_{\text{ET}}$  and  $W_{\text{BT}}$  symbols represent the energy transfer and back-transfer rates. The calculate values of these quantities are presented in Table 1. The  $\Phi$  and  $K$  symbols represent the non-radiative decay rates. Typical values of the

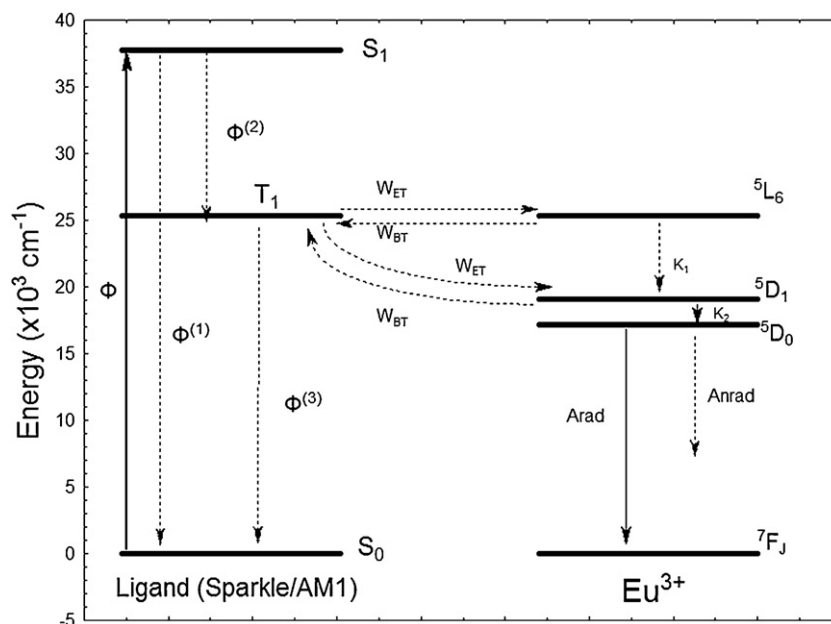


Fig. 3. Schematic representation of the energy transfer mechanism used to treat the energy transfer process in the studied complexes.

remaining transfer rates were assumed to be identical to those found for coordination compounds, namely,  $\Phi = 10^4$ ,  $\Phi^{(1)} = 10^6$ ,  $\Phi^{(2)} = 10^8$ , and  $\Phi^{(3)} = 10^5 \text{ s}^{-1}$  [44].

### 3. Results and discussions

#### 3.1. Analysis of the energy transfer rates

Singlet and triplet energies for all complexes studied are presented in Table 1.

The main effects as well as the interaction effects obtained from the factorial planning can be observed in Fig. 4. The main effect R1 is associated with the change of the  $\text{NO}_2$  by  $\text{NH}_2$  in the R1 position; the main effect R2 is associated with the change of the hydrogen by  $\text{CH}_3\text{CH}_2$  in the R2 position and the main effect R3 is

associated with the change of the  $\text{CH}_3$  by  $\text{CF}_3$  in the R3 position. The interaction effects are associated with simultaneous changes in respective positions. For example the interaction effect R1R3 is associated with the interaction between the simultaneous substitutions of the  $\text{NO}_2$  by  $\text{NH}_2$  in the R1 position and of the  $\text{CH}_3$  by  $\text{CF}_3$  in the R3 position. The same observation can be used in the analyses of Fig. 6.

It can be observed that the main effect R3 is the most important one and that the interaction effects R1R2 and R1R2R3 are small compared to the others. As the results were obtained via quantum chemistry calculations, it was not possible to have a measure of the pure error. Thus all the calculated effects were considered in the analysis.

Energy transfer rates obtained for all complexes can be seen in Fig. 5, which shows the effect of different levels of the factors on

Table 1

Triplet energies and energies transfer and retro-transfer rates obtained for the eight studied complexes generated by the  $2^3$  factorial design.

	Ligand states ( $\text{cm}^{-1}$ )	4f states ( $\text{cm}^{-1}$ )	$R_L^a$ (Å)	$\Delta E$ ( $\text{cm}^{-1}$ )	Transfer rate ( $\text{s}^{-1}$ ) ( $W_{ET}$ )	Back-transfer rate ( $\text{s}^{-1}$ ) ( $W_{BT}$ )
Comp01	Singlet (38515)					
	Triplet (27491)→	$^5D_1$ (19070)	4.478	8421.4	$3.81 \times 10^7$	$1.43 \times 10^{-10}$
Comp02	Triplet (27491)←	$^5D_4$ (27600)	4.478	108.6	$1.654 \times 10^5$	$9.86 \times 10^4$
	Singlet (38843)					
Comp03	Triplet (30183)→	$^5D_1$ (19070)	3.818	11113	$1.022 \times 10^7$	0
	Triplet (30183)→	$^5D_4$ (27600)	3.818	2583	$2.908 \times 10^6$	13.11
Comp04	Singlet (37181)					
	Triplet (30816)→	$^5D_1$ (19070)	3.641	11746	$1.809 \times 10^6$	0
Comp05	Triplet (30816)→	$^5D_4$ (27600)	3.641	3216	$3.3 \times 10^6$	0.731
	Singlet (35779)					
Comp06	Triplet (27703)→	$^5D_1$ (19070)	5.0	8633	$1.8 \times 10^7$	$2.45 \times 10^{-11}$
	Triplet (27703)→	$^5D_4$ (27600)	5.0	103	$7.68 \times 10^5$	$4.70 \times 10^5$
Comp07	Singlet (37065)					
	Triplet (27278)→	$^5D_1$ (19070)	4.02	8208	$3.482 \times 10^8$	$3.601 \times 10^{-9}$
Comp08	Triplet (27278)←	$^5D_4$ (27600)	4.02	322	$3.148 \times 10^5$	$6.797 \times 10^4$
	Singlet (37726)					
Comp09	Triplet (25278)→	$^5D_1$ (19070)	4.149	6208	$8.168 \times 10^8$	$1.162 \times 10^{-4}$
	Triplet (25278)←	$^5L_6$ (25325)	4.149	47	$2.52 \times 10^6$	$2 \times 10^6$
Comp10	Singlet (35783)					
	Triplet (28465)→	$^5D_1$ (19070)	3.901	9395	$7.886 \times 10^7$	$2.861 \times 10^{-12}$
Comp11	Triplet (28465)→	$^5D_4$ (27600)	3.901	865	$3.3 \times 10^6$	$5.36 \times 10^4$
	Singlet (35799)					
Comp12	Triplet (26512)→	$^5D_1$ (19070)	3.999	7442	$7.123 \times 10^8$	$2.833 \times 10^{-7}$
	Triplet (26512)←	$^5G_6$ (26752)	3.999	240	$7.58 \times 10^5$	$2.42 \times 10^5$

<sup>a</sup>  $R_L$  is the distance from the donor state located at the organic ligands and the  $\text{Eu}^{3+}$  ion nucleus.

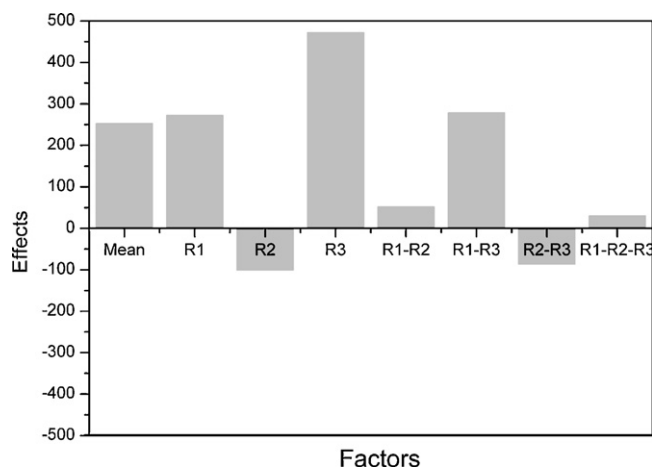


Fig. 4. Effects obtained for energy transfer rates.

the energy transfer rate. It is clear that the energy transfer rate from the triplet state of the ligand to  $^5D_1$  excited state of europium (III) ion is considerably increased by the presence of  $CF_3$  at R3 position. Also, the substitution of  $NO_2$  by  $NH_2$  at the R1 position generally increases the energy transfer rates, except for the structure with H at R2 and  $CH_3$  at R3 positions. Finally, it was found that the presence of  $CH_2CH_3$  at R2 only favors the energy transfer rate if R1 and R3 position were occupied by  $NH_2$  and  $CH_3$  groups, respectively.

In summary, combination of  $CF_3$  group (strong acceptor) at R3 position and the presence of the  $NH_2$  group (strong donor) at R1 position greatly favors the energy transfer rate. It is important to emphasize that the presence of a hydrogen atom at R2 position also contributes to an increase in the energy transfer rates in most of the cases. Therefore, the highest energy transfer rate is presented by the complex labelled Comp06, which has  $NH_2$ , H and  $CF_3$  groups at R1, R2 and R3 positions.

### 3.2. Quantum yield analyses

Quantum yield values, populations for  $^5D_0$  level of europium (III) ion and for the ground state ( $S_0$ ) of the ligands for all complexes generated by factorial planning  $2^3$  are presented in Table 2. In order to support the discussion on those results, we shall rely on the results of the factorial planning.

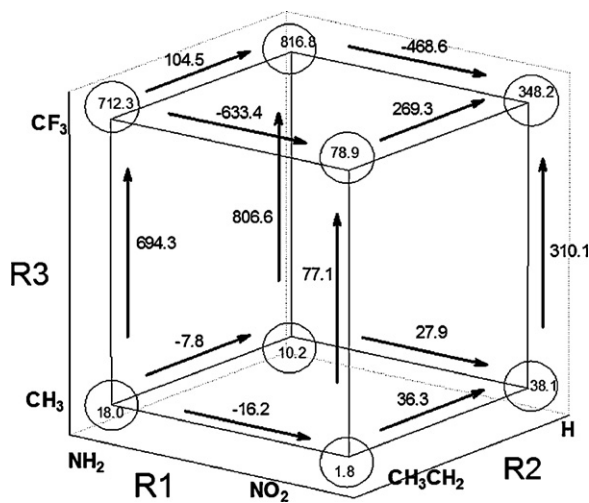


Fig. 5. Graphic visualization of the influence of the substituents groups in R1, R2 and R3 positions in the energy transfer rates from triplet to  $^5D_1$  ( $Eu^{3+}$ ) state. All values are divided by  $10^6$ .

Table 2

Quantum yields, populations of  $^5D_0$  level of europium (III) ion and populations of ground state ( $S_0$ ) of the ligands for all complexes generate by the  $2^3$  factorial design.

Population of $^5D_0$ state	Ground state population ( $S_0$ )	Quantum yield (%)
Comp01 0.84745	0.15131	56.01
Comp02 0.79868	0.19984	39.96
Comp03 0.69772	0.30039	23.23
Comp04 0.81983	0.17890	45.83
Comp05 0.87192	0.12685	68.74
Comp06 0.87370	0.12507	69.86
Comp07 0.86194	0.13678	63.02
Comp08 0.86430	0.13432	64.34

The main effects and the interaction effects of the substitutions on the quantum yields from the factorial planning are represented graphically in Fig. 6. Analogously to the energy transfer rate analysis, the main effect R3 is the most significant one, but in this case R1R2 and R1R2R3 interaction effects are higher than the others. All the main and interaction effects were used for the analysis for the same reasons stated for the energy transfer rate.

The effect of the substitution of  $NH_2$  by  $NO_2$  depends on the nature of the substituents present at the remaining positions, as evidenced by the graphical visualization of the effects, Fig. 7. For instance, when the  $NH_2$  substitution by  $NO_2$  takes place in a substrate containing H and  $CH_3$  at R2 and R3 positions respectively, the quantum yield increases by 16%. On the other hand for a substrate containing  $CH_3CH_2$  and  $CH_3$  at R2 and R3 positions, the quantum yield increase upon  $NH_2$  substitution was found to be 22.6%. Nevertheless the highest quantum yield can be found when H and  $CF_3$  groups are present at the R2 and R3 positions, respectively.

Analogously to the trend observed in the transfer rate results, the presence of  $CF_3$  group at R3 position plays a similar role in determining the magnitude of quantum yield, since a significant increase in quantum yield was observed for all  $CF_3$ -containing structures. In contrast to the  $CF_3$  role, the presence of  $CH_3CH_2$  at R2 position barely affects the quantum yield: this substitution can be advantageous only if the structure contains  $NH_2$  at R1 and  $CH_3$  at R3 position. Quantum yield analysis also pointed out that structures bearing a strong donor such as  $NH_2$  will exhibit a high quantum yield. This analysis reproduces the general conclusion outlined

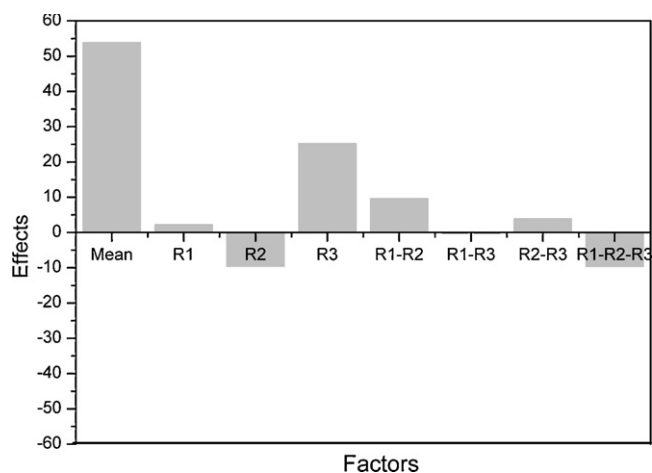


Fig. 6. Effects obtained for quantum yields.

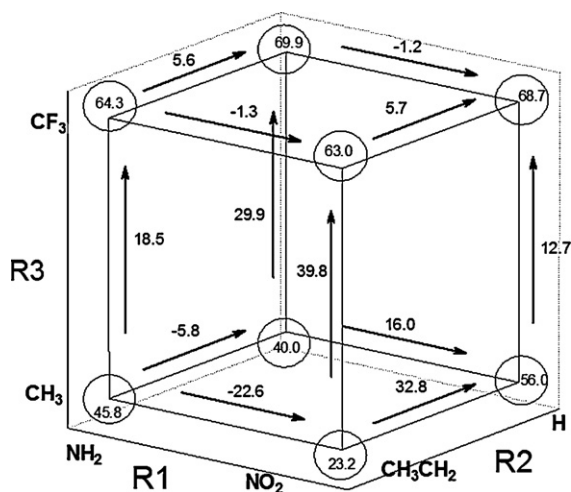


Fig. 7. Graphic visualization of the influence of the substitutes groups in R1, R2 and R3 positions in the quantum yields.

from energy transfer rate: high quantum yields are favoured by combination of a strong acceptor at R3 and strong donor at R1. However, the substitution of NH<sub>2</sub> by NO<sub>2</sub> almost had no effect on the quantum yield whatever the group is at R2 (H or CH<sub>2</sub>CH<sub>3</sub>).

#### 4. Conclusions

A comparative analysis of the results indicates the possibility of obtaining structures with simultaneously high energy transfer rates and quantum yields based on substitutions at R1 position of  $\beta$ -diketone ligands by a strong acceptor and at R3 by a strong donor. According to the 2<sup>3</sup> factorial planning results, the less significant substitution was at R2 position. The only significant effect of R2 substitution was the slight increase in quantum yield for the case of H substituent. Although it may seem disadvantageous to substitute H for CH<sub>3</sub>CH<sub>2</sub> considering the quantum yield, the solubility in organic solvents is expected to increase upon the substitution. Moreover, as the difference in the quantum yield for the most efficient complexes with H (Comp06) and CH<sub>3</sub>CH<sub>2</sub> (Comp08) at R2 position is only 5.6%, the comp08 complex can be a suitable choice to deposition in the form of films. Finally, as the comp06 structure exhibited a quantum yield close to 70%, it would be a good candidate to application in light converting molecular devices.

#### Acknowledgments

We appreciate the financial support from CNPq and CAPES (Brazilian agencies) and Brazilian Molecular and Interfaces Nanotechnology Network (RENAMI). We also wish to thank Centro Nacional de Processamento de Alto Desempenho (CENAPAD) at Campinas, Brazil, for having made available to us their computational facilities. The authors are grateful to Prof. A.E. Almeida Paixão for the use of Statistica. Finally, we gratefully acknowledge the Cambridge Crystallographic Data Centre for the Cambridge Structural Database 2008.

#### References

- [1] J.-M. Lehn, Perspectives in supramolecular chemistry—from molecular recognition towards molecular information processing and self-organization, *Angew. Chem. Int. Ed. Engl.* 29 (1990) 1304–1309.
- [2] D.L. Taylor, A.S. Waggoner, R.F. Murphy, F. Lanni, R.R. Birge, Applications of Fluorescence in Biomedical Sciences, A.R. Liss Inc., New York, 1986.
- [3] G. Mathis, Rare-earth cryptates and homogeneous fluoroimmunoassays with human sera, *Clin. Chem.* 39 (1993) 1953–1959.
- [4] C. Lopez, B. Alpha, G. Mathis, Europium(III) trisbipyridine cryptate label for time-resolved fluorescence detection of polymerase chain-reaction products fixed on a solid support, *Clin. Chem.* 39 (1993) 196–201.
- [5] G. Mathis, Probing molecular-interactions with homogeneous techniques based on rare-earth cryptates and fluorescence energy-transfer, *Clin. Chem.* 41 (1995) 1391–1397.
- [6] T. Soukka, K. Antonen, H. Härmä, A.-A. Pelkkikangas, P. Huhtinen, T. Lövgren, Highly sensitive immunoassay of free prostate-specific antigen in serum using europium(III) nanoparticle label technology, *Clin. Chim. Acta* 328 (2003) 45–58.
- [7] M.F. Tweedle, J.C.G. Bünzli, G.R. Choppin, Lanthanide Probes In Life Chemical, and Earth Science, Elsevier, Amsterdam, 1989, Chapter 5.
- [8] K. Kumar, M.F. Tweedle, Macrocyclic polyaminocarboxylate complexes of lanthanides as magnetic-resonance-imaging contrast agents, *Pure Appl. Chem.* 65 (1993) 515–520.
- [9] R.O. Freire, F.R.G. Silva, M.O. Rodrigues, M.E. Mesquita, N.B.C. Júnior, Design of europium (III) complexes with high quantum yield, *J. Mol. Model.* 12 (2005) 16–23.
- [10] R.O. Freire, R.Q. Albuquerque, S.A. Júnior, G.B. Rocha, M.E. Mesquita, On the use of combinatory chemistry to the design of new luminescent Eu<sup>3+</sup> complexes, *Chem. Phys. Lett.* 405 (2005) 123–126.
- [11] O.L. Malta, F.R. Gonçalves e Silva, A theoretical approach to intramolecular energy transfer and emission quantum yields in coordination compounds of rare earth ions, *Spectrochim. Acta A* 54 (1998) 1593–1599.
- [12] M.O. Rodrigues, N.B.C. Júnior, C.A. Simone, A.A.S. Araujo, A.M. Brito-Silva, F.A.A. Paz, M.E. Mesquita, S.A. Júnior, R.O. Freire, Theoretical and experimental studies of the photoluminescent properties of the coordination polymer [Eu(DPA)(HDPA)(H<sub>2</sub>O)<sub>2</sub>]-4H<sub>2</sub>O, *J. Phys. Chem. B* 112 (2008) 4204–4212.
- [13] O. Eisenstein, L.J. Maron, DFT studies of some structures and reactions of lanthanides complexes, *Organomet. Chem.* 647 (2002) 190–197.
- [14] X. Cao, M. Dolg, Density functional studies on lanthanide (III) texaphyrins (Ln-Tex(2+), Ln = La, Gd, Lu): structure, stability and electronic excitation spectrum, *Mol. Phys.* 101 (2003) 2427–2435.
- [15] U. Cosentino, A. Villa, D. Pitea, G. Moro, V. Barone, A. Maiocchi, Conformational characterization of lanthanide(III)-DOTA complexes by ab initio investigation in vacuo and in aqueous solution, *J. Am. Chem. Soc.* 124 (2002) 4901–4909.
- [16] L. Perrin, L. Maron, O. Eisenstein, Modelling Me<sub>5</sub>C5 for reactivity studies in (eta(5)-C<sub>5</sub>Me<sub>5</sub>)<sub>2</sub>Ln-R: full DFT and QM/MM approaches, *New J. Chem.* 10 (2004) 1255–1259.
- [17] M. Dolg, H. Stoll, A. Savin, H. Preuss, Energy-adjusted pseudopotentials for the rare-earth elements, *Theor. Chim. Acta* 75 (1989) 173–194.
- [18] T.R. Cundari, W. Stevens, Effective core potential methods for the lanthanides, *J. Chem. Phys.* 98 (1993) 5555–5565.
- [19] R.O. Freire, G.B. Rocha, R.Q. Albuquerque, A.M. Simas, Efficacy of the semiempirical sparkle model as compared to ECP ab-initio calculations for the prediction of ligand field parameters of europium (III) complexes, *J. Lumin.* 111 (2005) 81–87.
- [20] R.O. Freire, G.B. Rocha, A.M. Simas, Lanthanide complex coordination polyhedron geometry prediction accuracies of ab-initio effective core potential calculations, *J. Mol. Model.* 12 (2006) 373–389.
- [21] A.V.M. de Andrade, N.B. Costa, A.M. Simas, R.L. Longo, O.L. Malta, G.F. de Sa, Methodology for the theoretical design of light conversion molecular devices, *Quim Nova* 21 (1998) 51–59.
- [22] M.E. Mesquita, S.A. Junior, F.C. Oliveira, R.O. Freire, N.B. Costa Jr., G.F. de Sa, Synthesis, spectroscopic studies and structure prediction of the new Tb(3-NH<sub>2</sub>pic)<sub>3</sub>-3H<sub>2</sub>O complex, *Inorg. Chem. Comm.* 5 (2002) 292–295.
- [23] M.E. Mesquita, S.A. Junior, N.B. Costa Jr., R.O. Freire, R.F.G. Silva, G.F. de Sa, Synthesis, Sparkle Model, intensity parameters and spectroscopic studies of new Eu(fod)<sub>3</sub>phen-NO complex, *J. Solid State Chem.* 171 (2003) 183–188.
- [24] R. Pavithran, M.L.P. Reddy, S. Alves Jr., R.O. Freire, G.B. Rocha, P.P. Lima, Synthesis and luminescent properties of novel europium(III) heterocyclic  $\beta$ -diketone complexes with Lewis bases: structural analysis using Sparkle/AM1 Model, *Eur. J. Inorg. Chem.* 20 (2005) 4127–4129.
- [25] R.O. Freire, G.B. Rocha, A.M. Simas, Sparkle model for the calculation of lanthanide complexes: AM1 parameters for Eu(III), Gd(III) and Tb(III), *Inorg. Chem.* 44 (2005) 3299–3310.
- [26] R.O. Freire, N.B. Costa Jr., G.B. Rocha, A.M. Simas, Sparkle/AM1 structure modeling of lanthanum (III) and lutetium (III) complexes, *J. Phys. Chem. A* 110 (2006) 5897–5900.
- [27] R.O. Freire, N.B. Costa Jr., G.B. Rocha, A.M. Simas, Sparkle/AM1 parameters for the modeling of samarium (III) and promethium (III) complexes, *J. Chem. Theory Comput.* 2 (2006) 64–74.
- [28] R.O. Freire, N.B. Costa Jr., G.B. Rocha, A.M. Simas, Modeling lanthanide coordination compounds: Sparkle/AM1 parameters for praseodymium (III), *J. Organomet. Chem.* 690 (2005) 4099–4102.
- [29] R.O. Freire, G.B. Rocha, A.M. Simas, Modeling rare earth complexes: Sparkle/AM1 parameters for thulium (III), *Chem. Phys. Lett.* 411 (2005) 61–65.
- [30] N.B. Costa Jr., R.O. Freire, G.B.G.B. Rocha, A.M. Simas, Sparkle model for the AM1 calculation of dysprosium (III) complexes, *Inorg. Chem. Commun.* 8 (2005) 831–835.
- [31] C.C. Bastos, R.O. Freire, G.B. Rocha, A.M. Simas, Sparkle model for AM1 calculation of neodymium (III) coordination compounds, *J. Photochem. Photobiol. A* 117 (2006) 225–237.
- [32] R.O. Freire, G.B. Rocha, A.M. Simas, Sparkle/PM3 for the modeling of europium(III), gadolinium(III), and terbium(III) complexes, *J. Braz. Chem. Soc.* 20 (2009) 1638–1645.

- [33] G.E.P. Box, W.G. Hunter, J.S. Hunter, *Statistics for Experimenters*, first ed., Wiley, New York, 1978.
- [34] R.E. Bruns, I.S. Scarminio, B.B. Neto, *Statistical Design–Chemometrics*, first ed., Elsevier Science, London, 2006.
- [35] G.R. Choppin, J.-C.G. Bünzli, *Lanthanoid Probes in Life, Medical and Environmental Science*, Elsevier, Amsterdam, 1989.
- [36] J.-C.G. Bünzli, J.-M. Pfefferlé, Bovine alpha-lactalbumin—identification of 2 metal-ion-binding sites using the europium(III) luminescent probe, *Helv Chim. Acta* 77 (1994) 323–333.
- [37] F.H. Allen, The Cambridge structural database: a quarter of a million crystal structures and rising, *Acta Crystallogr. B* 58 (2002) 380–388.
- [38] I.J. Bruno, J.C. Cole, P.R. Edgington, M. Kessler, C.F. Macrae, P. McCabe, J. Pearson, R. Taylor, New software for searching the Cambridge structural database and visualizing crystal structures, *Acta Crystallogr. B* 58 (2002) 389–397.
- [39] F.H. Allen, W.D.S. Motherwell, Applications of the Cambridge Structural Database in organic chemistry and crystal chemistry, *Acta Crystallogr. B* 58 (2002) 407–422.
- [40] J.J.P. Stewart, in: S.C. Chemistry (Ed.), MOPAC2007, Version 7.058, Colorado Springs, USA, 2007.
- [41] J.E. Ridley, M.C. Zerner, Triplet-states via intermediate neglect of differential overlap—benzene, pyridine and diazines, *Theor. Chim. Acta* 42 (1976) 223–236.
- [42] M.C. Zerner, G.H. Loew, R.F. Kirchner, U.T. Mueller-Westerhoff, Intermediate neglect of differential—overlap technique for spectroscopic of transition-metal complexes—ferrocene, *J. Am. Chem. Soc.* 102 (1980) 589–599.
- [43] M.C. Zerner, ZINDO Manual, QTP, University of Florida, Gainesville, FL, 1990, p. 32611.
- [44] O.L. Malta, F.R.G. Silva, R.L. Longo, *Chem. Phys. Lett.* 307 (1999) 518–526.